



Lyotropic liquid crystallinity in mixed-tautomer Schiff-base macrocycles

Journal:	<i>ChemComm</i>
Manuscript ID	CC-COM-07-2015-006253.R1
Article Type:	Communication
Date Submitted by the Author:	11-Sep-2015
Complete List of Authors:	Jiang, Jian; UBC, Chemistry Department Dong, Ronald Y.; University of British Columbia, Department of Physics and Astronomy MacLachlan, Mark; UBC Chemistry, Chemistry Department

Lyotropic liquid crystallinity in mixed-tautomer Schiff-base macrocycles

Received 00th January 20xx,
Accepted 00th January 20xx

Jian Jiang,^a Ronald Y. Dong^b and Mark J. MacLachlan^{*,a}

DOI: 10.1039/x0xx00000x

www.rsc.org/

Schiff-base macrocycles that combine keto-enamine and enol-imine tautomers within the same ring were synthesized and characterized. These new macrocycles form host-guest complexes with organic cations and unexpectedly form a lyotropic liquid crystal in organic solvents such as chloroform and toluene.

Salen (and its analogues) is one of the most important ligands in coordination chemistry, especially for catalysis and supramolecular chemistry.^{1,2} Shape-persistent conjugated macrocycles incorporating salen-type components can be conveniently formed by the condensation of aldehydes and amines,³⁻⁷ and these macrocycles are interesting for host-guest chemistry,^{8,9} nanofiber assembly,¹⁰ and as hosts for metal oxide clusters and molecular magnetic materials.¹¹ Considering that many Schiff-base macrocycles have disc-shaped geometries reminiscent of discotic mesogens, the potential of these substances to form liquid crystals is great. Yet, few examples of Schiff base macrocycles that form thermotropic liquid crystals have been reported,¹² and, to the best of our knowledge, no examples of lyotropic liquid crystals based on these molecules have been discovered.

With oxygen donor atoms in their interiors, Schiff-base macrocycles such as **1** (Fig. 1) can complex organic cations (e.g., **4-7**).⁹ Assemblies between Schiff-base macrocycles and guests were primarily held together by electrostatic interactions. In addition, by comparing the binding constant of guests, π - π interactions were found to play an important role in the host-guest assembly. Modification of the π -basic cavity of Schiff-base macrocycles was expected to improve the binding properties of the macrocyclic host.

Macrocycle **2** was previously prepared and found to be predominantly the keto-enamine form.¹³ Incorporation of

naphthalene into the structure of macrocycle **1** was expected to form a similar keto-enamine structure, instead of enol-imine tautomer. Here we report the synthesis and characterization of new Schiff-base macrocycles that combine keto-enamine and enol-imine tautomers in the same ring. The macrocycle can be used as supramolecular host and forms a lyotropic liquid crystal in organic solvents.

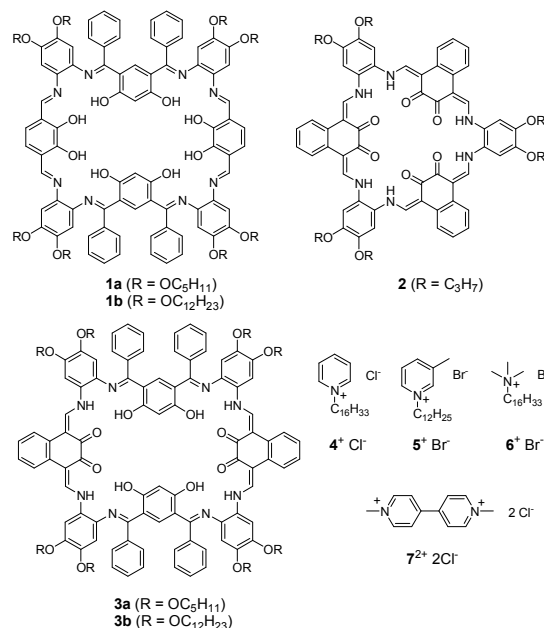


Fig. 1 The structure of macrocycles **1-3** and ions investigated as potential guests

Macrocycles **3a** and **3b** were synthesized in 35 and 41% yield, respectively, through a sequence of ketimine formation followed by aldimine formation (see ESI). The structures of the macrocycles were verified by mass spectrometry, IR spectroscopy, elemental analysis, and NMR spectroscopy. In the ¹H NMR spectrum of **3a**, there are two doublets at 14.67 and 8.76 ppm, which are attributed to the resonance of NH (H_a in structure **3a** in Fig. 2) and enamine protons (H_b in structure of **3a** in Fig. 2), respectively. A ¹H-¹H COSY NMR spectrum of **3a**

^a Department of Chemistry, University of British Columbia, 2036 Main Mall, Vancouver, BC, Canada V6T 1Z1. mmaclach@chem.ubc.ca

^b Dept. of Physics and Astronomy, University of British Columbia, 6224 Agriculture Rd., Vancouver, BC, Canada V6T 1Z1.

† We thank NSERC for funding (Discovery Grant)

Electronic Supplementary Information (ESI) available: Synthesis and characterization of **1b**, **3a**, and **3b**; supporting spectra, Job plots, mass spectra, modelling, and POM images. See DOI: 10.1039/x0xx00000x

shows strong J-coupling between H_a and H_f. Based on our previous experience, this J-coupling is only observed in the case of keto-enamine tautomers where there is an N-H bond.¹⁴ Tautomerization is not expected at the resorcinol rings as they have 1,3-diimino linkages.¹⁵ In support of this assignment, the resonance of the OH (resorcinol) is observed as a singlet at 14.85 ppm in CDCl₃. The IR spectrum also shows peaks assigned to both carbonyl and imine groups (1614 (C=O) and 1548 (C=N) cm⁻¹). Thus, the interior of the macrocycle presents both hydroxyl and carbonyl groups as shown in Fig. 1. Macrocycle **3b** also has the same arrangement of keto-enamine / enol-imine tautomers in its interior.

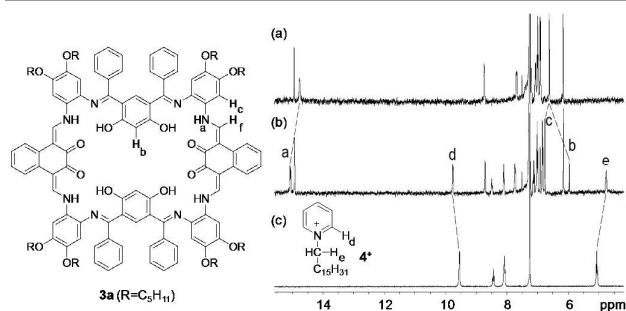


Fig. 2 ¹H NMR spectra of (a) macrocycle **3a**, (b) mixture of macrocycle **3a** and cetylpyridinium chloride **4⁺Cl⁻** ([**4⁺**]:[**1**] = 1.2:1), and (c) **4⁺Cl⁻** (400 MHz, CDCl₃, 298 K). NMR peaks are assigned as shown in the molecular structures.

Upon addition of organic cations, shifts of the resonances for the protons of both the macrocycle and cations were observed by ¹H NMR spectroscopy (Fig. 2), indicating the formation of host-guest complexes. The inclusion structure was also proved by a 2D-ROESY spectrum, which showed coupling between protons on the guest and protons inside of the macrocycle. Moreover, MALDI-TOF mass spectrometry verified the formation of 1:1 host-guest complexes and we observed significant changes in the UV-vis spectroscopy upon guest binding (see ESI).

Compared to **1a**, four hydroxyl groups are replaced by carbonyl groups in the interior of **3a**. Because the electronegativity of oxygen on a carbonyl group is smaller than that for a hydroxyl group (2.34 for carbonyl group¹⁶ and 2.8 for hydroxyl group¹⁷), it may be expected that the association constant for binding organic cations inside **3a** will be smaller than that by **1a**. NMR titration of cetyltrimethylammonium bromide (**6⁺Br⁻**) into both **1a** and **3a** verified this to be the case (Table S1). However, comparing titration results of pyridinium salts into **1a** and **3a** tells a different story - the binding constants of **4⁺** and **5⁺** with **3a** are higher than those with **1a**. We attribute the higher binding constants of **4⁺** and **5⁺** with **3a** to the better π-π interaction that is possible with the naphthalene groups.

In solution, the ¹H NMR spectrum of **3a** indicates that the molecule has C_{2v} symmetry, but this is likely an average structure. Semi-empirical (PM3) calculations show that there are many possible conformations of macrocycle **3a** with similar energies, which means that **3a** may be very flexible. The flexibility of macrocycle **3a** can be explained by its non-

conjugated structure that allows for twisting out of planarity with minimal energy penalty. Simulation of a complex formed between macrocycle **3a** and pyridinium (pyridinium ⊂ **3a**) shows the phenyl ring of pyridinium may interact, by π-π stacking, with the tautomerized naphthalene moiety of macrocycle **3a**, which can be shown in energy-minimized structures calculated for complex **4⁺ ⊂ 3a** (Fig. S27).

We expected that the extra methyl group on the aromatic head of **5⁺** would weaken the π-π interaction with the hosts when compared with **4⁺**. Steric hindrance was also expected to impede the inclusion of **5⁺**. However, the association constant for complex **5⁺ ⊂ 1a** is very similar to that of **4⁺ ⊂ 1a**, and the association constants of **5⁺ ⊂ 3a** and **4⁺ ⊂ 3a** are also similar (Table S1). This can be explained by the charge diffuse nature of guest **5⁺**. The similarity of these values is consistent with electrostatic forces between the cation and the electron-rich macrocycle dominating the association.

Job plots (see ESI) verified that 1:1 complexes are formed when **4⁺**, **5⁺** and **6⁺** combine with macrocycle **3a**. Calculation of binding constant of NMR titration data by EQNMR¹⁸ shows experimental results fit very well with a 1:1 system. However, a Job plot shows that methyl viologen **7²⁺** binds macrocycle **3a** in a 2:1 (host:guest) proportion. In our previous work, we found viologens form a 1:1 complex with macrocycle **1a**.⁹ It is likely that intermolecular interactions in macrocycle **3a** favor dimerization, such that the macrocycle can bind methyl viologen in a 2:1 complex. Enhanced π-π stacking between tautomerized naphthalene moieties and/or intermolecular hydrogen bonding between carbonyl and NH groups may facilitate this dimerization tendency.

We were very surprised to discover that macrocycle **3b** forms a lyotropic liquid crystal in relatively non-polar solvents. When **3b** was dissolved in toluene or chloroform, strong aggregation was evident by ¹H NMR spectroscopy (see ESI). In particular, as the concentration was increased, the peaks associated with the macrocycle underwent substantial broadening, correlating with a decreased T₂ relaxation time and increased size from molecular association. Modelling indicated that the ketimine phenyl rings orient in a way that prevents the macrocycles from stacking directly one on top of the other (Fig. 3a) and block the formation of a columnar assembly. Therefore, we believe that the aggregation may be attributed to the lateral packing of molecules.

When a concentrated sample of **3b** in toluene was sandwiched between an untreated glass slide and a glass cover slip, an interesting Schlieren texture with roughly parallel stripes was observed with a polarized optical microscope (POM), Fig. 3b. The domains of the Schlieren texture are separated by clear walls.

Although lyotropic mesophases are very difficult to characterize by X-ray diffraction (XRD), we obtained an XRD pattern for a sample of **3b** in toluene inside a capillary tube. The 2D XRD pattern of a sample (Fig. 3c) showed two peaks on the meridian with maxima at d = 12.5 and 6.2 Å, likely indicative of layer ordering. The layer periodicity lies between the length (20 Å) and half-length of macrocycle **3b**, suggesting an interdigitated structure. Well-defined peaks on the

meridian indicate that the molecules spontaneously align within the capillary tube. The equatorial diffraction observed is a sharp peak with d-spacing of 27.3 Å in the small angle region, indicating the formation of another lamellar arrangement in which the layer normal is perpendicular to the direction of capillary tube. Based on the 2D XRD data and the dimensions of macrocycle **3b**, we propose an interdigitated lamellar structure, such as that shown in Fig. 3d.

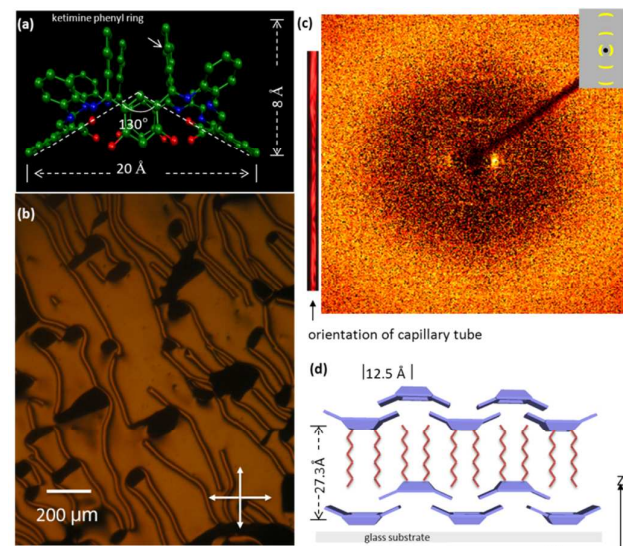


Fig. 3 (a) Cone conformation of **3b** (side view). (Simulated with semi-empirical calculation (PM3) with Spartan'04, alkyl chains were removed for clarity). (b) The optical textures of a sandwiched sample of **3b**/toluene (40 wt% **3b**) at 22 °C, observed with crossed polarizers. (c) The 2D diffraction pattern of **3b**/toluene (40 wt% **3b**) measured in a 0.1 mm capillary at 23 °C (Inset: sketch of the X-ray diffraction pattern). (d) Proposed sketch of molecular packing of the lamellar phase when viewed along the Y axis.

To further probe the nature of the lyotropic phase, we undertook a deuterium (^2H) NMR study of **3b** in toluene- d_8 (40 wt% **3b**) between 293 and 333 K (Fig. 4). The spectra clearly show an aligned phase, in which the disc-normal director of the macrocycles is oriented perpendicular to the external magnetic field, similar to discotic mesogens. Three quadrupolar splittings are discernible from the spectra: a larger one corresponding to the para deuterium, a smaller one with higher intensity assigned to ortho/meta deuterons, and an intermediate one from the methyl deuterons. Toluene's ring plane is aligned along the field direction in the liquid crystal, and the order parameter S of the toluene's planar normal is estimated to vary between 0.032 and 0.023 based on the quadrupolar splittings. Rotating the sample at ambient temperature by 90° about an axis normal to the NMR magnetic field produced a ^2H powder spectrum that correlates to a planar distribution of the directors.

If our model with interdigitation of the macrocycles is correct, then naphthalene-naphthalene interactions should be important to stabilize the lyotropic liquid crystal. To test whether the naphthalene moiety of macrocycle **3b** was necessary for the formation of a liquid crystal, macrocycle **1b** with benzene rings in the place of naphthalene was

synthesized. No liquid crystallinity was observed for macrocycle **1b** in toluene. Since the main difference between **3b** and **1b** is the absence of naphthalene moieties in the structure of **1b**, we believe that the longer naphthalene moieties play a central role in stabilizing the lyotropic liquid crystal. We did not observe lyotropic liquid crystallinity in **3a**, indicating that the substituents have a role in stabilizing the liquid crystalline state, or at least providing enough solubility to reach the concentrations necessary to observe the liquid crystallinity.

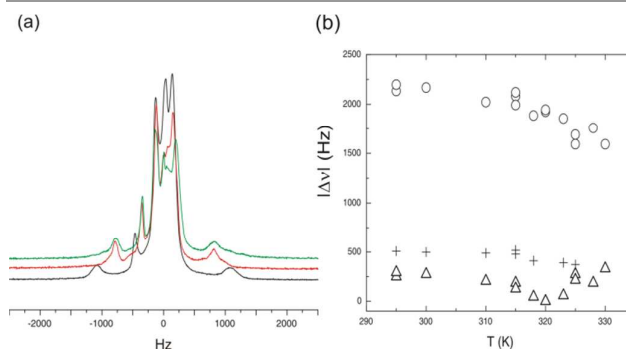


Fig. 4 (a) ^2H NMR spectra of **3b**/toluene- d_8 in the lamellar phase at 300, 325 and 330 K (increasing from the bottom trace) (30.72 MHz; a solid echo pulse sequence¹⁹ with 90° pulse width of 3.3 μs was used to collect the spectra.). (b) Plot of absolute quadrupolar splittings vs. temperature. Note that the smallest splitting passes through zero as the CD bond angle for ortho/meta deuterons is close to the magic angle (Legend: o para deuterium, Δ ortho/meta deuterons, + methyl deuterons).

We observed an interesting transformation of the liquid crystal (**3b**/toluene (40 wt% **3b**)) under relatively low light intensity. When the light intensity of the POM increased above the minimum intensity needed to view the texture ($\sim 100 \text{ mW/m}^2$ at 560 nm), we observed a grid texture in the LC phase, thus confirming the fluidity of the phase. As the light intensity increased to 230 mW/m^2 , bubbles several micrometers in diameter appeared superimposed on the original Schlieren texture (Fig. 5d). Above 450 mW/m^2 light intensity, the bubbles transformed into squares that assembled into a grid pattern (Fig. 5a). From the images, it is clear that the squares are actually formed by a grid pattern of perpendicular stripes. By slightly rotating the polarizer in each direction, the opposite coloration of the perpendicular components could be observed (Fig. 5b,c). Fig. 5d-f shows the transformation of the original Schlieren texture to the grid pattern. Note that the process is reversible: upon removing the light source, the striped Schlieren texture returns to the sample. Further increase of the light intensity of the POM resulted in an oscillatory grid pattern with the squares expanding until the birefringent texture disappeared (see ESI). Both polarized and unpolarized light could induce the grid pattern. As well, light with different frequencies in the visible spectrum (obtained using optical filters) trigger the grid pattern formation at similar intensity within experimental error. The pattern-formation process may likely be thermal due to light absorption since increasing the temperature (to 27 °C when light intensity was fixed at 100 mW/m^2) also triggered

the formation of the grid pattern. The thermal sensitivity of the liquid crystallinity may arise because of the conformational flexibility of the macrocycle. DSC experiments showed no phase transitions from -10 to 40 °C for **3b**/toluene (40 wt% **3b**).

Liquid crystallinity was also observed for **3b** in chloroform and dichloroethane at concentrations greater than about 30 wt% **3b**. Fig. S29 shows representative textures observed by POM.

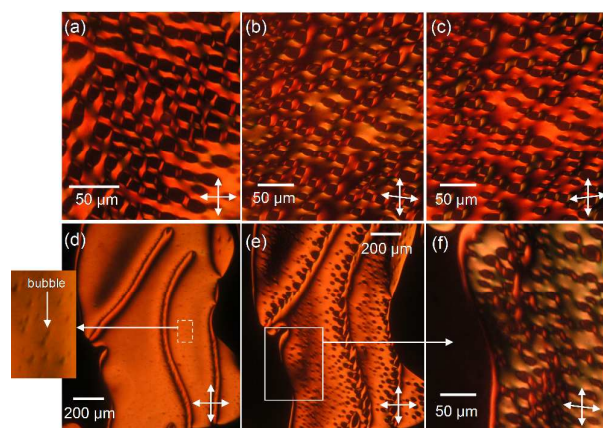


Fig. 5 (a), (b) and (c) Optical photomicrographs of grid pattern of **3b**/toluene (40 wt% **3b**) at 22 °C, in which textures were observed under crossed polarizers, with the polarizers rotated ca. 10° clockwise and with the polarizers rotated ca. 10° counter-clockwise, respectively (light intensity of POM is about 450 mW/m² at 560 nm). (d), (e) Formation of grid pattern in a domain of the Schlieren texture, in which the light intensity was set at 230 and 450 mW/m² for (d) and (e), respectively. The bubbles formed in the domain are shown on the left of (d). (f) Close-up view of texture in (e) with ca. 10° clockwise rotation of the polarizer.

Conclusions

We have synthesized Schiff-base macrocycles that combine enol-imine and keto-enamine tautomers in a single ring. The macrocycles bind organic cations in their interiors, as deduced by NMR titration experiments, mass spectrometry, and ROESY-NMR spectra. Most surprisingly, these macrocycles with long alkyl chains form lyotropic liquid crystalline phases in organic solvents such as toluene and chloroform. The combination of POM, XRD, and ²H NMR spectroscopy suggest that the mesophase formed is a lamellar phase of relatively high viscosity, but further verification of the specific phase will be pursued. These macrocycles cannot arrange in a stack like discotics, and their formation of a lyotropic liquid crystal is unexpected. Considering the substantial interest in lyotropic liquid crystals for organizing materials on different length scales,²⁰ we hope that this report will open up additional research efforts to investigate lyotropic liquid crystals in organic solvents.

Notes and references

- 1 C. J. Whiteoak, G. Salassa and A. W. Kleij, *Chem. Soc. Rev.*, 2012, **41**, 622; Y. E. Lee, T. Cao, C. Torruellas and M. C.

- 2 Kozłowski, *J. Am. Chem. Soc.*, 2014, **136**, 6782; N. Maudoux, T. Roisnel, V. Dorcet, J. F. Carpentier and Y. Sarazin, *Chem.-Eur. J.*, 2014, **20**, 6131; L. Hussein, N. Purkait, M. Biyikal, E. Tausch, P. W. Roesky and S. Blechert, *Chem. Commun.*, 2014, **50**, 3862; R. M. Clarke and T. Storr, *Dalton Trans.*, 2014, **43**, 9380.
- 3 M. A. Lebedeva, T. W. Chamberlain and E. S. Davies, *Chem.-Eur. J.*, 2013, **19**, 11999; Z. Y. Guo, S.-M. Chan and C. W. Michael, *Chem.-Eur. J.*, 2013, **19**, 8937; P. K. Dutta, S. Panda and G. R. Krishna, *Dalton Trans.*, 2013, **42**, 476; C. P. Pradeep and S. K. Das, *Coord. Chem. Rev.*, 2013, **257**, 1699.
- 4 N. E. Borisova, M. D. Reshetova and Y. A. Ustynyuk, *Chem. Rev.*, 2007, **107**, 46; P. A. Vigato, S. Tamburini and L. Bertolo, *Coord. Chem. Rev.*, 2007, **251**, 1311; M. J. MacLachlan, *Pure Appl. Chem.*, 2006, **78**, 873.
- 5 A. J. Gallant and M. J. MacLachlan, *Angew. Chem. Int. Ed.*, 2003, **42**, 5307; C. Ma, A. Lo, A. Abdolmaleki and M. J. MacLachlan, *Org. Lett.*, 2004, **6**, 3841; P. D. Frischmann, J. Jiang, J. K.-H. Hui, J. J. Grzybowski and M. J. MacLachlan, *Org. Lett.*, 2008, **10**, 1255; J. K.-H. Hui and M. J. MacLachlan, *Chem. Commun.*, 2006, 2480; S. Guieu, A. K. Crane and M. J. MacLachlan, *Chem. Commun.*, 2011, **47**, 1169.
- 6 S. Akine, T. Taniguchi and T. Nabeshima, *Tetrahedron Lett.*, 2001, **42**, 8861; S. Akine, S. Sunaga and T. Nabeshima, *Chem. Eur. J.*, 2011, **17**, 6853.
- 7 D. J. de Geest, A. Noble, K. S. Murray, D. S. Larsena and S. Brooker, *Dalton Trans.*, 2007, 467; J. Gao, R. A. Zingaro, J. H. Reibenspies and A. E. Martell, *Org. Lett.*, 2004, **6**, 2453; J. Gawronski, M. Kwit, J. Grajewski, J. Gajewy and A. Długokinska, *Tetrahedron: Asymmetry*, 2007, **18**, 2632; G. Salassa, A. M. Castilla and A. W. Kleij, *Dalton Trans.* 2011, **40**, 5236.
- 8 G. Givaja, M. Volpe, M. A. Edward, A. J. Blake, C. Wilson, M. Schröder and J. B. Love, *Angew. Chem. Int. Ed.*, 2007, **46**, 584; J. B. Love, *Chem. Commun.*, 2009, 3154; H. Shimakoshi, H. Takemoto, I. Aritome and Y. Hisaeda, *Tetrahedron Lett.*, 2002, **43**, 4809.
- 9 J. Jiang and M. J. MacLachlan, *Org. Lett.* 2010, **12**, 1020.
- 10 J. Jiang and M. J. MacLachlan, *Chem. Commun.*, 2009, 5695.
- 11 J. K.-H. Hui, P. D. Frischmann, C.-H. Tso, C. A. Michal and M. J. MacLachlan, *Chem. Eur. J.*, 2010, **16**, 2453.
- 12 P. D. Frischmann and M. J. MacLachlan, *Chem. Commun.*, 2007, 4480; P. D. Frischmann, G. A. Facey, P. Y. Ghi, A. J. Gallant, D. L. Bryce, F. Lejl and M. J. MacLachlan, *J. Am. Chem. Soc.*, 2010, **132**, 3893; A. J. Gallant, J. H. Chong and M. J. MacLachlan, *Inorg. Chem.*, 2006, **45**, 5248; T. Nabeshima, H. Miyazaki, A. Iwasaki, S. Akine, T. Saiki, C. Ikeda and S. Sato, *Chem. Lett.*, 2006, **35**, 1070; L. Cuesta, E. Tomat, V. M. Lynch and J. L. Sessler, *Chem. Commun.*, 2008, 3744; H. L. C. Feltham, F. Kloewer, S. A. Cameron, D. S. Larsen, Y. Lan, M. Troiano, S. Faulkner, A. K. Powell and S. Brooker, *Dalton Trans.*, 2011, **40**, 11425; H. L. C. Feltham, R. Clerac, A. K. Powell and S. Brooker, *Inorg. Chem.*, 2011, **50**, 4232.
- 13 S.-i. Kawano, Y. Ishida and K. Tanaka, *J. Am. Chem. Soc.*, 2015, **137**, 2295.
- 14 A. J. Gallant, M. Yun, M. Sauer and M. J. MacLachlan, *Org. Lett.*, 2005, **7**, 4827.
- 15 J. H. Chong, M. Sauer, B. O. Patrick and M. J. MacLachlan, *Org. Lett.*, 2003, **5**, 3823.
- 16 M. Sauer, C. Yeung, J. H. Chong, B. O. Patrick and M. J. MacLachlan, *J. Org. Chem.*, 2006, **71**, 775.
- 17 R. E. Kagarise, *J. Am. Chem. Soc.*, 1955, **77**, 1377.
- 18 A. F. Clifford, *J. Phys. Chem.*, 1959, **63**, 1227.
- 19 M. J. Hynes, *J. Chem. Soc., Dalton Trans.*, 1993, 311.
- 20 J. H. Davis, K. R. Jeffrey, M. Bloom, M. Valic and T. P. Higgs, *Chem. Phys. Lett.*, 1976, **42**, 390.
- 21 C. Wang, D. Chen and X. Jiao, *Sci. Technol. Adv. Mater.*, 2009, **10**, 023001.